J Solid State Electrochem (2012) 16:2365–2372
DOI 10.1007/s10008-011-1583-5

ORIGINAL PAPER

Silver nanoparticles electrooxidation: theory and experiment

Kh. Z. Brainina · L. G. Galperin · T. Yu. Kiryuhina · A. L. Galperin · N. Yu. Stozhko · A. M. Murzakaev · O. R. Timoshenkova

Received: 20 September 2011 / Revised: 18 October 2011 / Accepted: 24 October 2011 / Published online: 13 November 2011

Abstract This article presents the findings of microscopic and electrochemical studies of electrooxidation of silver nanoparticles of varying sizes in comparison with "bulk" silver. Silver particles were immobilized on the surface of indifferent carbon-containing screen-printed electrodes. Vacuum-deposited silver represented the "bulk" electrode. The calculations and experimental studies demonstrated that the transition from macro- to nanostructural electrodes is followed by a shift of the maximum current potential of metal oxidation into the area with more negative potentials. A positive correlation between experimental and calculated data confirms once again a relevant application of the earlier proposed mathematical model and the possible use of the shift of the maximum current potential of electrooxidation to describe the electrochemical activity and surface energy properties of metal nanoparticles.

Keywords Mathematical modeling · Silver · Nanoparticles · Size effect · Electrochemical oxidation · Electron microscopy

The authors dedicate this paper to the 75th birthday of Dr. Nina Zakharchuk and wish her many years of health, luck, and success.

K. Z. Brainina (✉) · T. Y. Kiryuhina · N. Y. Stozhko
Ural State University of Economics,
8 Marta St, 62,
Ekaterinburg 620144, Russia
e-mail: baz@usue.ru

K. Z. Brainina · L. G. Galperin · A. L. Galperin
Ural Federal University,
Mira St 19, A-203,
Ekaterinburg 620002, Russia

A. M. Murzakaev · O. R. Timoshenkova
Institute of Electrophysics,
Ural Branch of the Russian Academy of Science,
Amundsen St, 106,
Ekaterinburg 620016, Russia

Introduction

The interaction of electrochemistry and nanotechnology has two sides, namely, application of nanotechnology in electrochemistry and vice versa as was correctly stated by Ali Eftekhari in "Preface" of [1]. Electrochemistry of metal nanostructures is of particular interest due to their special properties which are different from those of microcrystalline and bulk samples, namely: lower melting point [2], catalytic and adsorptive activity [3], and better sensory properties [4–6].

In the ongoing development of biosensors, the use of nanotechnology and nanomaterials has raised new possibilities of controlling properties of transducers, matrices for immobilization of biomolecules: markers, indicators, and other important building components. Among a variety of nanoparticles, metallic gold and silver are the most often used materials in sensor preparation. One of the main quantitative characteristics of nanoparticles is Gibbs free surface energy. It differs significantly from energy for macroobjects. Electrochemistry can become one of the tools to resolve the problem connected with the lack of comprehensive theoretical and experimental data. Probably, the first researchers who observed electrooxidation of silver nanocrystals immobilized on the bulk silver were Krebbs and Roe [7]. Later, the effect was described in some works [8–12].

Redmond et al. [8], following the approach proposed by Plieth [13], used Eq. 1:

$$E^0{}_{\mathrm{np}} = E^0{}_{\mathrm{bulk}} - (2\gamma v_{\mathrm{M}})/zFr \quad (1)$$

(γ—the surface tension, v_{M}—the molar volume, z—the lowest valence state, F—Faraday's constant, r—the radius) to describe the standard electrode potential $E_{\mathrm{np}}{}^0$ of small metal particle shifts to more negative area in comparison with the value for bulk metal $E_{\mathrm{bulk}}{}^0$.

Table 1 Parameters for the calculation of silver particle electrooxidation voltammograms

Parameter	Value
M, silver molar mass	107.8 $gmol^{-1}$
ρ, silver density	10.5 gcm^{-3}
σ, surface tension of silver on the boundary with air at 970 °C [15]	800 dyn cm^{-1}
n, number of electrons participating in the electrode process	1
δ, fraction of particles of a particular size	Relative unit
E^0, standard electrode potential of Ag^+/Ag, vs. $Ag^+/AgCl$ sat. el.	0.589 V
ΔG^0, Gibbs free surface energy	J mol^{-1}
r^0, radius of the particles under investigation	nm

The authors suppose that the negative shift in the standard electrode potential of small particles means that smaller metal nanoparticles are more easily oxidized than bulk material.

Ivanova and Zamborini [14] noted that E_p shifts to more positive area with increasing Ag^+/Ag seed ratio (or increasing particle size). They think that the shift in E_p is a result of a size-dependent change in E^0 for the Ag/Ag^+ redox couple.

The distinction of our earlier proposed approach [10] consists in taking into account the surface free Gibbs energy impact into the electrooxidation process thermodynamics and kinetics. Numerical simulation [10] and voltamperometric investigation of nanoparticles electrooxidation [11, 12] demonstrated validity of assumptions and existence of interrelation between Gibbs free surface energy of the particles and the potential of maximum oxidation current. The calculations and experimental studies showed that the transition from macro- to nanostructured electrode is followed by a shift of the maximum current potential of metal oxidation into the area with more negative potentials, which correlates with Gibbs free surface energy of the particles and their size. The physical and mathematical model and calculations performed were discussed in our previous papers [10–12]. The results of quantitative comparison of calculated and experimental data for gold and bismuth nanoparticles electrooxidation are given in [11, 12]. The introduction of Gibbs free surface energy $\Delta G^0 = \sigma S$ (σ—surface tension, S—molar surface of nanoparticles) into the calculations enabled one to obtain good agreement between theoretical and experimental data while studying the electrooxidation of gold [11] and bismuth [12] nanostructures. The continuation of these studies with silver is essential as it allows one not only to obtain new data regarding kinetics of silver electrooxidation but also to add new evidence of feasible use of easily obtained electrochemical data as a source of information about such thermodynamic parameters of metal nanostructures as Gibbs free surface energy.

Calculated data

The parameters used to obtain a series of calculated silver electrooxidation voltammograms are given in Table 1.

All the parameters used in the calculations are reference values with the exception of Gibbs free surface energy,

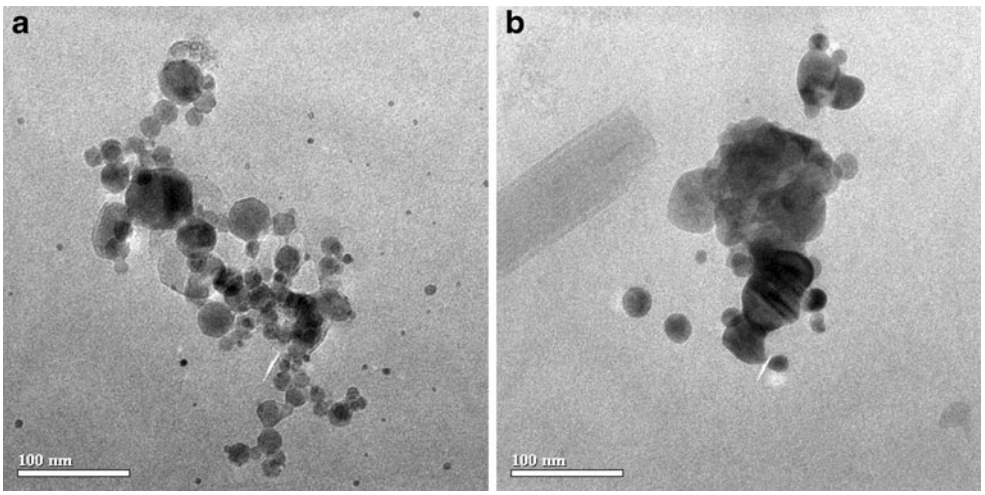

Fig. 1 TEM images of silver nanoparticles: **a** yellow sol, **b** red sol

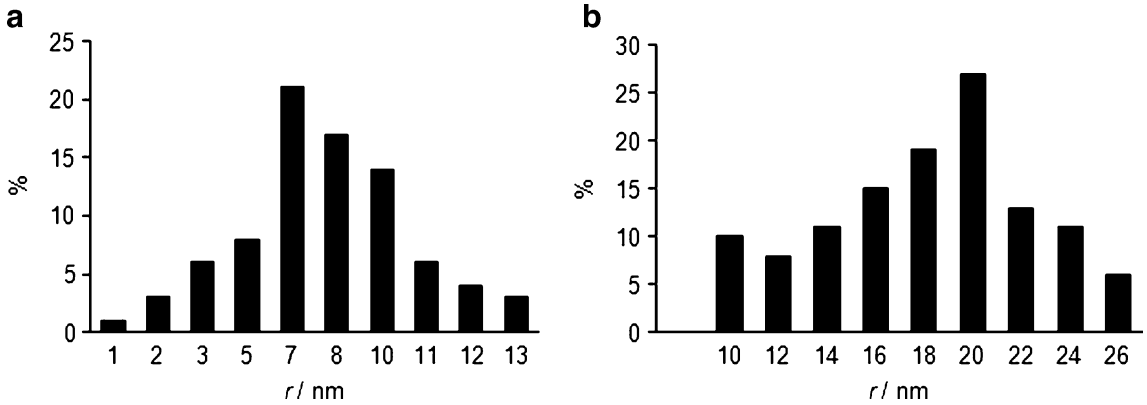

Fig. 2 Distribution of silver particles by size in **a** yellow and **b** red sols

ΔG^0, and the constant of electrode process rate, k_s. The value of ΔG^0 was calculated as:

$$\Delta G^0 = \sigma \times S_M \quad (2)$$

$$S_M = 3M/\rho r^0 \quad (3)$$

where S_M—surface area of 1 mol of the studied particles of a given size.

In order to determine the value of k_s, a series of voltammogramms for the "bulk" electrode was calculated with various k_s. The voltammograms were compared with the experimental curve which shows electrooxidation of "bulk" silver. Then, the calculated curve coinciding with the experimental one was selected. The value of k_s for this curve was used for further calculations. Properties of the "bulk" electrode were modeled by specifying in the calculation the particle radius of 1 μm and taking into account the fact that particles of this size have the properties of macrostructures.

Experimental section

Materials, instruments, and methods

Microscopic studies of silver sols were performed with the transmission electron microscope (TEM) JEM 2100 (JOEL, Japan). The scanning electron microscope LEO 982 (Carl Zeiss, Germany) was used to characterize nanoparticle size and distribution on the electrode surface.

Silver sols were dispersed for 1–2 min with the ultrasonic processor VCX 750 (Sonics & Materials, Inc. USA) at a capacity of 300 W. Deionized water with resistivity not exceeding 18 MΩ cm was obtained with the reverse osmosis unit UVOI-MF (Russia). Silver nanoparticles were synthesized with the use of the magnetic stirrer with heating IKA RCT (Germany). The vacuum universal post VUP-4 (JSC Nasosenergomash—Sumy, Ukraine) was used to deposit silver on the polymer substrate. Linear sweep voltammetry served as a main measurement method. The semiautomatic inverse voltammetric analyzer interfaced to a personal computer IVA-5 (Russia) and a three-electrode electrochemical cell were used for electrochemical investigation. A glassy carbon rod served as auxiliary electrode; a saturated silver/silver chloride electrode (Metrohm, Switzerland) served as reference electrode. All potentials are given relative to this electrode. Carbon screen-printed electrodes with the working surface area of 0.10 cm^2 (IVA Ltd. Russia) were used as working electrodes. Ink CIRCALOC 6971 (Lord, USA) and Cementit-CH-3172 (Niederwangen, Switzerland) were used as carbon containing material and insulator.

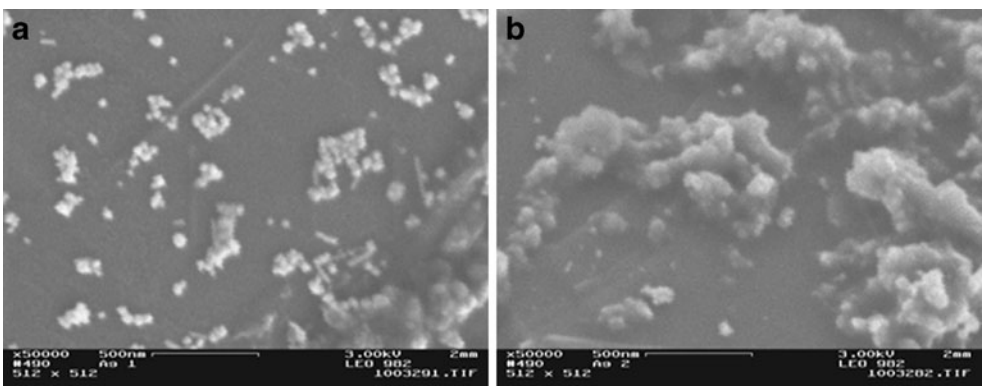

Fig. 3 SEM images of silver nanoparticles: **a** yellow concentrated sol, **b** red concentrated sol (×100,000, LEO 982)

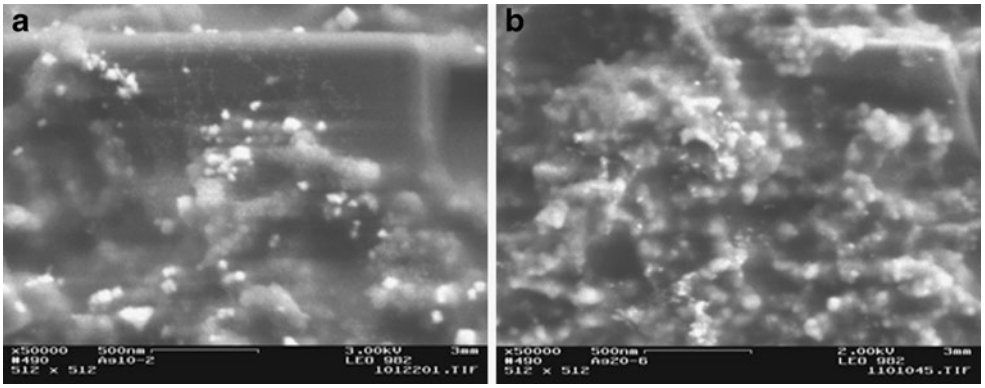

Fig. 4 SEM images of silver nanoparticles: **a** yellow diluted sol, **b** red diluted sol (×100,000, LEO 982)

The reagents—sodium citrate (Na-cit) (Labtech, Russia), silver nitrate ($AgNO_3$) (Reaktiv, Russia), potassium nitrate (KNO_3) (Reakhim, Russia), hydrate hydrazine (N_2H_5OH) (Reakhim, Russia), acids H_2SO_4 (Sigma Tech, Russia), and HNO_3 (JSC Azot, Russia)—were of "high" and "extra high" purity grade. All solutions were prepared using deionizied water. All laboratory glassware were carefully treated with concentrated acids (H_2SO_4, HNO_3) and rinsed well with deionized water.

Preparation of electrodes

Screen-printed electrodes were modified with silver nanoparticles. For this purpose, 7 μL of sol was placed on the working surface of the electrode and left at room temperature in open air until completely dry. The bulk silver electrode was manufactured by metal sputtering from the wire surface (d=0.2 mm) onto polyethyleneterephthalate substrate of 0.25 mm thickness. The deposited silver layer was 0.5–1.0 μm in thickness.

A certain surface area of the electrode was separated so that during dissolution of metal the amount of electricity consumed should be similar to the amount consumed during the oxidation of nanoparticles. The excess surface was isolated.

Synthesis of silver nanoparticles

Silver nanoparticles were synthesized by chemical reduction of $AgNO_3$ with N_2H_5OH in the presence of Na-cit by adapting the method introduced in [16].

Yellow sol was obtained by adding freshly prepared cit-Na to a boiling solution containing 1×10^{-3} M $AgNO_3$ with vigorous stirring (1,200 rpm) for 4–5 min. Then, the sol was cooled to room temperature in a dark place. Yellow sol was obtained with C($AgNO_3$)/C(Na-cit) =1:4.

Synthesis of red sol was carried out by adding freshly prepared Na-cit and N_2H_5OH to a solution containing 1×10^{-3} M $AgNO_3$/[C($AgNO_3$)/C(Na-cit)/C(N_2H_5OH)=1:4:1] at 25 °C for 2 min with vigorous stirring (1,200 rpm). Then, the sol was cooled to room temperature in a dark place.

Silver sols with varying concentrations were prepared by diluting concentrated sol.

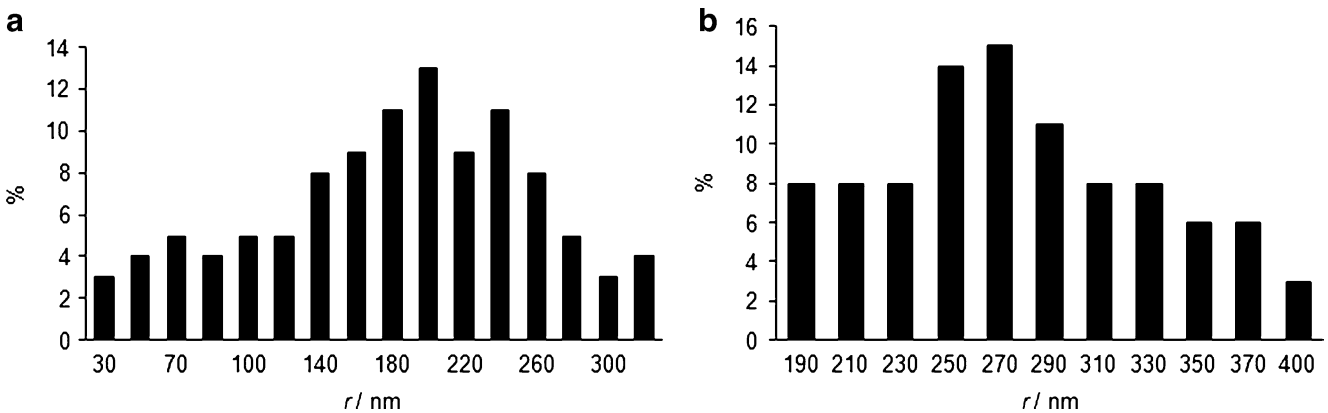

Fig. 5 Distribution of silver particles by size on electrodes modified with concentrated **a** yellow and **b** red sols

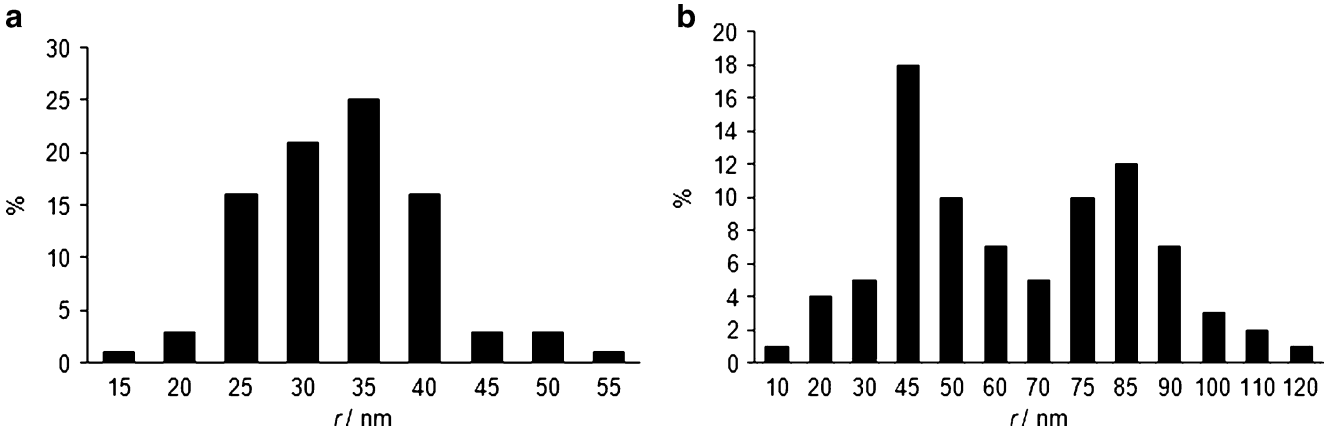

Fig. 6 Distribution of silver particles by size on electrodes modified with diluted **a** yellow and **b** red sols

Results and discussion

Characterization of silver nanoparticles

Nanoparticles in the sol

Figure 1 shows the TEM images of synthesized silver sols. It can be observed that the silver particles have spherical shape. Both individual particles and their agglomerates are present in the sol. Figure 2 shows the distribution of nanoparticles by size in yellow and red sols. The sol contains particles of different sizes—from 1 to 13 nm in the yellow sol (the weighted average particle radius is 7 nm) and from 10 to 26 nm in the red sol (the weighted average particle radius is 20 nm).

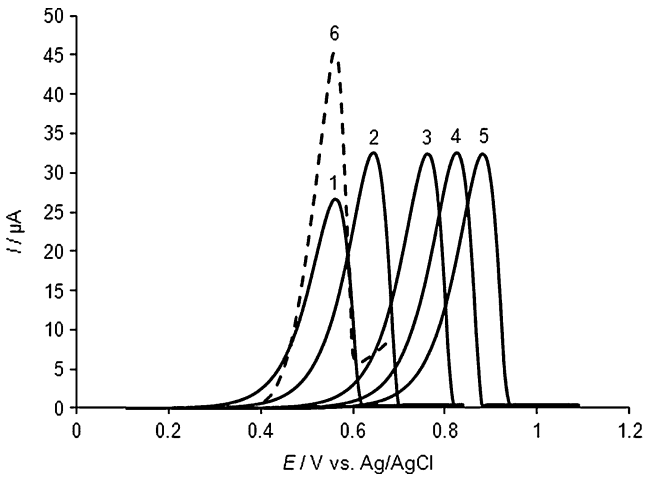

Fig. 7 Experimental and calculated voltammograms for bulk silver electrode electrooxidation. Background: 0.1 M KNO_3, υ=0.05 Vs^{-1}. Calculation parameters: r=1 μm; Q=63.6 μC; ΔG^0=25.718 $Jmol^{-1}$; δ=1; k_S=5×10^{-6} (*1*, *6*); 1×10^{-6} (*2*); 1×10^{-7} (*3*); 3×10^{-8} (*4*); 1×10^{-8} (*5*) cm s^{-1}. Other parameters are given in Table 1. *6* is experimental voltammogram

Nanoparticles on the electrode surface

Figures 3 and 4 show SEM images of the electrode surface modified with concentrated yellow and red sols and three-time diluted sols, respectively. The surface of the electrodes is not homogeneous. Silver particles immobilized on the surface are seen as white spots. Both individual particles of silver and their agglomerates are present. The number of agglomerates on the electrodes modified with concentrated sols is significantly higher than that on the electrodes modified with diluted sols.

Figures 5 and 6 characterize the particle distribution by size as obtained by analyzing 35 images in each case. It is apparent from Fig. 5 that in the concentrated yellow sol the average radius of particles is 200 nm (distribution is from 30 to 350 nm) and in the diluted yellow sol is 35 nm. In the concentrated red sol, the weighted average radius of particles is 270 nm (distribution is from 190 to 400 nm), while the diluted red sol is characterized by a mixture of nanoparticles with two dominant sizes—45 and 85 nm. It should be noted that there is significant difference in the size of the particles in sols and on the electrode surface. The reason for the observed enlargement of particles is, apparently, agglomeration and, possibly, recrystallization during evaporation of water from the sol deposited on the electrode surface. The aforementioned values are used for further calculation of voltammograms of silver oxidation.

Nanoparticles electrooxidation

Voltammograms of silver electrooxidation are presented in Figs. 7 and 8. Used as background electrolyte was 0.1 KNO_3.

Figure 7 shows a series of voltammograms presenting silver electrooxidation from the surface of the "bulk"

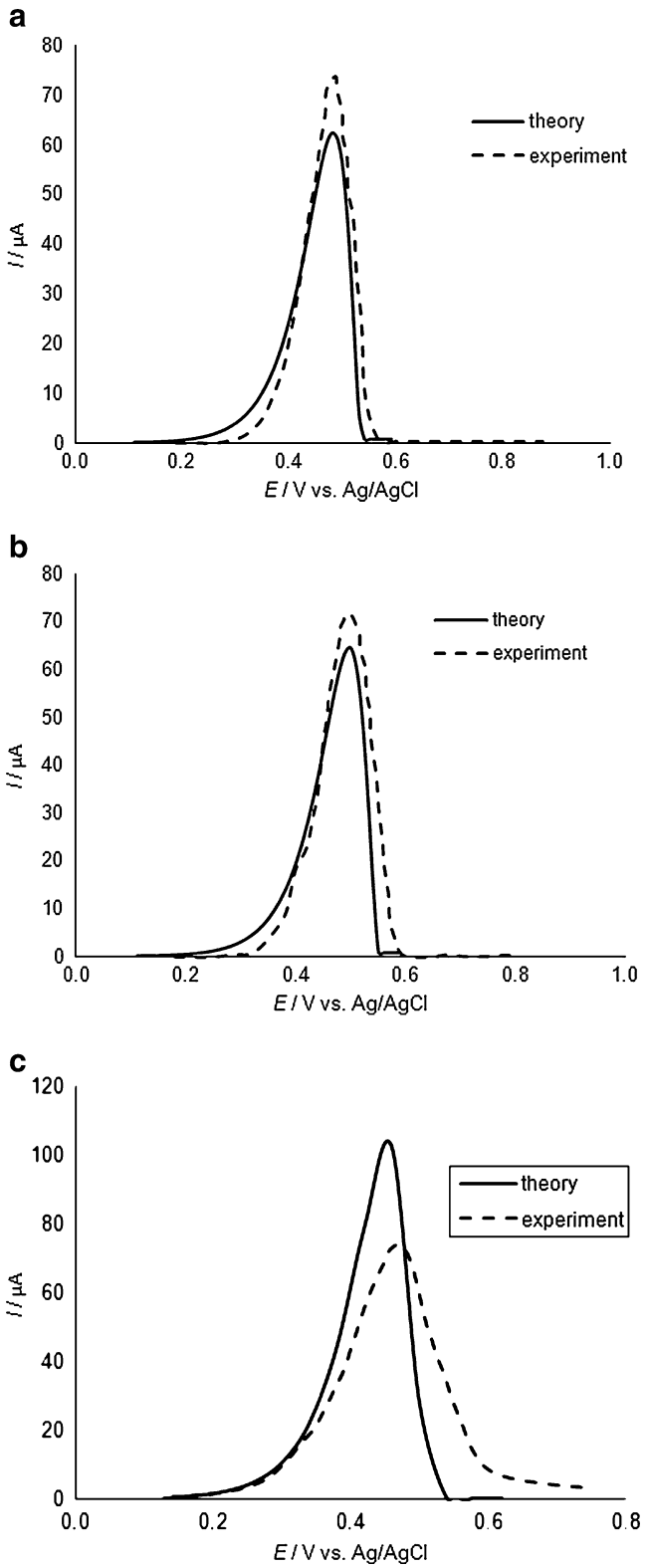

Fig. 8 Experimental and calculated voltammograms for silver nanoparticles electrooxidation. Background: 0.1 M KNO_3. Calculation parameters: δ=1; **a** r^0=200 nm, Q=144.4 μC, ΔG^0=128.6 Jmol^{-1}, υ=0.05 Vs^{-1}; **b** r^0=270 nm, Q=149.5 μC, ΔG^0=95.2 Jmol^{-1}, υ=0.05 Vs^{-1}; **c** r^0=35 nm, Q=59.2 μC, ΔG^0=734.8 Jmol^{-1}, υ=0.2 Vs^{-1}. Other parameters are given in Table 1

Table 2 Particle size effect on maximum current potential

r^0, nm	"bulk" electrode	270	35
E_{max}, V	0.563	0.498	0.469

electrode, calculated for different k_s values and the experimental curve. The signal of electrochemical oxidation of the "bulk" electrode is characterized by a clearly marked and easily measured peak of anodic current.

It is apparent from the figure that the voltammogram calculated for $k_s=5\times10^{-6}$ cm s^{-1} corresponds to the experimental curve. This value of k_s was used in subsequent calculations.

Figure 8 represents the experimental and calculated voltammograms of electrooxidation of silver nanoparticles of different sizes. The shape of experimental and calculated curves was the same. The signals of electrochemical oxidation of nanoparticles are characterized by a clearly marked and easily measured peak of anodic current as it is observed in the case of electrooxidation of "bulk" electrode. Decrease in particle size was followed by a shift in the silver electrochemical oxidation potential towards the more negative area. These data are illustrated in Table 2.

Some discrepancy between calculated and experimental voltammograms is caused by the fact that calculations are based on mathematical model describing electrooxidation of monodisperse set of nanoparticles. In reality, we had polydisperse systems (see Figs. 2, 5, and 6). Numerical simulation of the processes describing electrooxidation of a polydisperse set of nanoparticles will be given in one of the following papers. The observed discrepancy does not prevent to achieve the aim of this work, namely, to demonstrate the role of free Gibbs energy in nanoparticle electrochemistry. Good correlation between peak potentials of calculated and experimental curves confirms the correctness of the model used [10] as it was in the cases of Au [11] and Bi [12] nanoparticles.

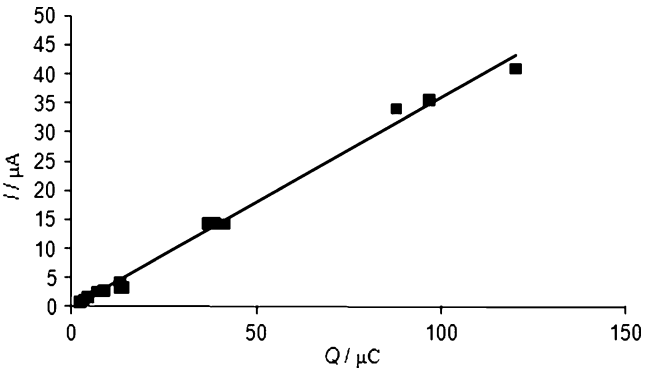

Fig. 9 Experimentally obtained I_m–Q dependence for nanoparticles 10 nm in size

Table 3 Calculated and experimental values of $d(\lg I)/d(\lg Q)$ (data for $r=10$ nm are given)

Parameter	Calculated value	Experimental value
$d(\lg I)/d(\lg Q)$	1.004	0.995

As a matter of fact, the observed discrepancy should not be considered as significant if we are to take into account the literature data spread, for example, silver surface tension, used in calculations.

Figure 9 shows the experimentally obtained I_m–Q dependence. It is linear. If we present the function $I = f(Q)$ as $I = kvQ$, then the parameter $d(\lg I)/d(\lg Q)$ will serve as the quantitative characteristic of dependence I–Q. Experimental and calculated values $d(\lg I)/d(\lg Q)$ are compared in Table 3. Good correspondence of the data given in Figs. 8 and 9 is obtained.

Below are calculations based on data given in [14]. Figure 10 presents voltammograms calculated using our model [10]. Table 4 includes the data taken from [14] and the results of our calculations.

The shape of the curves and their quantitative characteristics correlate with the experimental data obtained by the cited authors: they confirm once again the correctness of the thermodynamic approach used in our model for describing the electrochemistry of nanoparticles.

Conclusions

The results of the study of silver nanoparticle properties confirm the plausibility of electrochemical methods as source of information about electrooxidation kinetics and the value of Gibbs free surface energy.

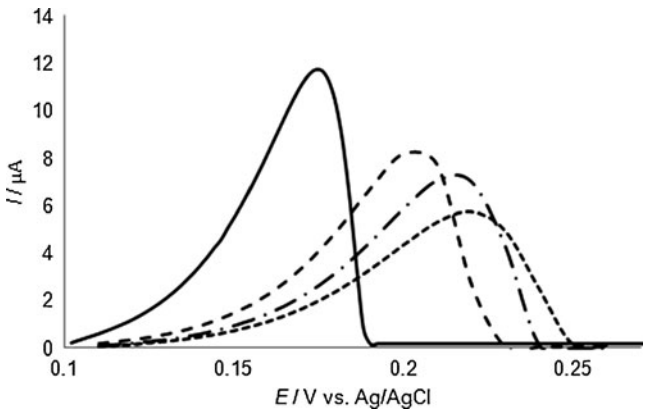

Fig. 10 Voltammograms calculated for $M=107.8$ gmol^{-1}, $E^0=0.59$ V, $\rho=10.5$ gcm^{-1}, $\sigma=835.0$ dyn cm^{-1}, $n=1.0$, $\upsilon=0.001$ Vs^{-1}, $\delta=1.0$, $r_{02}{}^0=1$ μM, $E_{in}=0.10$ V, $k_s=5\times10^{-6}$ cm s^{-1}, $r_{03}{}^0=4.25$, 9.45, 14.75, 18.9 nm (from the *left* to the *right*); Q was taken from Table 4

Table 4 Results of comparative analysis

d, nm [14]	$\Delta E_{1/2}$, V Experiment [14]	$\Delta E_{1/2}$, mV Calculation $k_s=5\times10^{-6}$ cm s^{-1}	I_{max}, μA Experiment [14]	I_{max}, μA Calculation $k_s=5\times10^{-6}$	Q 10^4, C Experiment [14]
8.5	33	32	17.5	10.7	4.3
18.9	48	37	6.8	8.0	3.9
29.5	54	52	8.0	7.0	3.8
39.8	65	50	7.0	5.4	3.3

$\Delta E_{1/2}$-peak half width

The calculations and experimental studies demonstrated that the transition from macro- to nanostructured electrodes is followed by a shift of the maximum current potential of metal oxidation into the area with more negative potentials. A good correlation between the experimental and calculated data confirms once again a relevant application of the earlier proposed mathematical model and the possible use of the shift of the maximum current potential of electrooxidation to describe the electrochemical activity and surface energy properties of metal nanoparticles. The data can also be useful for explanation and prediction of nanoparticle behavior as transducers in electrochemical/biochemical sensors as demonstrated in [4, 17, 18].

It is worth mentioning a significant fact stated in previous [10–12] and present works: the difference in particle sizes in sols and on the electrode surface. The reason for the observed enlargement of particles is, apparently, agglomeration and, possibly, recrystallization during evaporation of water from the sol deposited on the electrode surface. This phenomenon must be taken into account when studying surface processes and interpreting data. Generally speaking, it is of great importance to be careful in experimental data concerning nanoparticle electrochemistry interpretation because at least two factors should be taken into account: properties of nanoparticles themselves and their interaction with the substrate [19]. This effect can cause a shift of maximum electrooxidation current into the positive direction [20]. So, we cannot agree with authors [20] who discovered the effect mentioned and interpreted it as a consequence of increase of nanoparticle stability in comparison with bulk metal.

Nanostructural materials have led to major advances in different fields including electrochemical supercapacitors, portable electronic devices, catalysis, and sensors. It seems essential to explore the possibility of obtaining any information on their properties. There is a good reason to believe that the approach described in previous works [10–12] and the present paper can be useful for obtaining additional information about the thermodynamics and electrochemistry of nanostructures.

References

1. Eftekhari A (ed) (2008) Nanostructured materials in electrochemistry. Wiley, Weinheim
2. Jiang Q, Zhang S, Zhao M (2003) Mater Chem Phys 82:225–227
3. Krutyakov YuA, Kudrinsky AA, Olenin AYu, Lisichkin GV (2008) Uspekhi khimii 77:242–269
4. Stozhko NYu, Malakhova NA, Byzov IV, Brainina KhZ (2009) J Anal Chem 64:1176–1185
5. Welch CM, Compton RG (2006) Anal Bioanal Chem 384:601–619
6. Shtikov SN, Rusanova TYu (2008) Russ Chem Bull 52:92–100
7. Krebbs WM, Roe DK (1967) J Electrochem Soc 114:192–196
8. Redmond PL, Hallock AJ, Brus LE (2005) Nano Lett 5:131–135
9. Jones SEW, Campbell FW, Baron R, Xiao L, Compton RG (2008) J Phys Chem 112:17820–17827
10. Brainina KhZ, Galperin LG, Galperin AL (2010) J Solid State Electrochem 14:981–988
11. Brainina KhZ, Galperin LG, Vikulova EV, Stozhko NYu, Murzakaev AM, Timoshenkova OR, Kotov YuA (2011) J Solid State Electrochem 15:1049–1056
12. Brainina KhZ, Galperin LG, Piankova LA, Stozhko NYu, Myrzakaev AM, Timoshenkova OR (2011) J Solid State Electrochem. doi:10.1007/s10008-011-1455-z
13. Plieth WJ (1982) J Phys Chem 86:3166–3172
14. Ivanova OS, Zamborini FP (2010) J Am Chem Soc 132:70–72
15. Nikolskiĭ BP (ed) (1971) Spravochnik khimika, vol 1. Khimiâ, Moskva
16. Dadosh T (2009) Mater Lett 63:2236–2238
17. Vikulova EV, Malakhova NA, Stozhko NYu, Kolydina LI, Brainina KhZ (2011) Chem Sens 1:7–20
18. Uimin MA, Ermakov AE, Brainina KhZA (2010) J Anal Chem 65:640–647
19. Brainina Kh, Neiman E (1993) Electroanalytical stripping methods. Wiley, New York
20. Lakbub J, Pouliwe A, Kamasah A, Sun P (2011) Electroanalysis 23:2270–2274